(Preprint) AAS 12-136

APPROACHING MOONS FROM RESONANCE VIA INVARIANT MANIFOLDS

Rodney L. Anderson*

In this work, the approach phase from the final resonance of the endgame scenario in a tour design is examined within the context of invariant manifolds. Previous analyses have typically solved this problem either by using numerical techniques or by computing a catalog of suitable trajectories. The invariant manifolds of a selected set of libration orbits and unstable resonant orbits are computed here to serve as guides for desirable approach trajectories. The analysis focuses on designing an approach phase that may be tied into the final resonance in the endgame sequence while also targeting desired conditions at the moon.

INTRODUCTION

Solving the endgame problem as part of a tour design for a spacecraft traveling around multiple moons has become key as missions to various moons are considered, and the problem has been approached using a variety of different methods. Various definitions exist for the endgame problem, but it typically includes the last several resonance transitions before the final approach to the desired moon. The resonance transition problem has been approached using two-body patched conic methods, V_∞ leveraging,[1–3] optimization techniques,[4–6] Tisserand criterion techniques,[7–10] twist maps,[11] and dynamical systems techniques.[12–22] Resonant orbits have been shown to be essential to obtain a deeper understanding of these trajectory scenarios. Bollt and Meiss[23] used the recurrence properties of chaotic dynamics to search for Earth-Moon transfers in the circular restricted three-body problem (CRTBP), and Schroer and Ott[24] reduced the time of flight for these transfers by targeting the invariant manifolds of unstable resonant orbits. Belbruno and Marsden proposed that the resonance transition of comets could be explained using the weak stability boundary.[25] The heteroclinic connections of libration orbits were then used to explain these resonance transitions by Lo and Ross,[26] and Koon, Lo, Marsden, and Ross,[12] while Howell, Marchand, and Lo[14] verified this transition mechanism numerically. Anderson and Lo further showed that the invariant manifolds of resonant orbits play an integral part in the resonance transitions seen in ballistic,[21,27] impulsive,[20] and low-thrust trajectories.[19] In addition to this, Lantoine, Russell, and Campagnola used unstable resonant orbits themselves rather than their invariant manifolds as initial guesses in an optimization algorithm for trajectories stepping through resonances to a moon.[6,28]

The final approach and capture phase has been analyzed primarily on a case by case basis in part because the characteristics of the final orbit, or loosely captured trajectory, around the desired moon can vary significantly depending on the particular application. The moon of interest for the majority of these studies has been Europa. The Europa Orbiter[29,30] design from 1999 (see Sweetser et al.[29] and Johannesen and D'Amario[30]) used Finlayson's PTool software[31] to compute the trajectory for the final approach. Finlayson's software has been integral to this approach to the problem, and it worked by precomputing a database of potential trajectories with desirable characteristics that were then tied into the rest of the tour trajectory. In 2011, a similar technique was used in Grebow, Petropoulos and Finlayson[32] to numerically search for trajectories approaching Europa. Lo[33] had observed in 2001 that some of the trajectories computed using the Mystic optimization software appeared to follow the invariant manifolds of periodic libration orbits,[4] and Grebow et al. also observed that some of their more desirable trajectories heuristically appeared to follow these invariant manifolds

*Member of Technical Staff, Jet Propulsion Laboratory, California Institute of Technology, 4800 Oak Grove Drive, M/S 301-121, Pasadena, CA 91109

of libration point orbits or other periodic orbits in the CRTBP. Koon, Lo, Marsden, and Ross examined approaches to the libration orbits near the moon.[34] The general escape problem was analyzed primarily with the desire to understand stability by Villac and Scheeres.[35] Kirchbach et al.[36] looked at capture and escape with the goal of understanding whether their analyzed trajectories intersected Europa or Jupiter. Anderson and Lo[37] briefly examined the approach problem by investigating the resonances that trajectories ending at Europa could originate from over a short time period. In that work, libration orbits and the resonances that the libration point orbit invariant manifolds could travel to were also examined for different energies.

This study focuses on the final approach to the moon or secondary body in the CRTBP, assuming that the spacecraft has already transitioned through the previous required resonances. The results presented here are intended to give a representation of the types of trajectories that are available for this final approach so that they may be tied into a trajectory transitioning through this previous set of resonances as needed for specific mission requirements. Given that the recent Planetary Science Decadal Survey[38] contained missions to several different possible moons, this study examines and compares approaches for a range of different systems. Several cases approaching planets are also included for comparison. The approach taken here is to compute the invariant manifolds of unstable periodic orbits to use as a guide to provide a deeper understanding of this final approach scenario from a geometric and visual perspective. One of the first questions that may be asked is what resonances must be reached at the end of the resonant sequence to set up the spacecraft for the final approach? A planar version of the Europa Orbiter (PEO) trajectory computed in Anderson and Lo[20] traveled through the 5:6 resonance as its final resonance before the final Europa approach. It was determined that the trajectory selected the proper energy to target the L_2 gateway (described by Conley[39]) as computed using the stable manifold of a Lyapunov orbit at that same energy. More distant resonances were not enclosed in the invariant manifolds of the Lyapunov orbit at this energy, and at other energies the Lyapunov orbit invariant manifolds did not reach as far as the 5:6 resonance. This immediately suggests that one technique for determining the resonances required for the final approach is to compute the Lyapunov manifolds over different Jacobi constants and determine the resonances that they reach. This procedure is performed for several different systems using Jacobi constants that would be expected to enclose a wider range of resonances in the first section. The Jacobi constant is then varied for sample systems to determine how the enclosed resonances change as the energy level of the trajectory changes. Other types of orbits such as distant retrograde orbits among others have been observed to be significant to the approach problem,[33] and they will be analyzed in the future. Different types of unstable resonant orbits are evaluated here for selected systems and energies to determine which ones are most useful or desirable for approach within this context. The ΔVs required for insertion into a 200 km altitude orbit are then computed using both the unstable manifolds of resonant and Lyapunov orbits for selected systems. The energies where trajectories exist that insert at periapse relative to Europa are used to provide an initial basis for understanding the trade between the Jacobi constant and ΔV. Characteristics such as the time of flight of these trajectories are then analyzed. The approach problem encompasses trajectories coming in for orbital insertion as well as landing and impact trajectories, so landing trajectories are explored within the context of the invariant manifolds of Lyapunov orbits. The results from this analysis provide a way to study the deformation of the invariant manifolds or the libration orbit gateway in the ephemeris problem, and an initial study using this technique is undertaken. In general the focus is on providing insight into the options available for final approach for different energies to allow the trajectory to be tied into an arbitrary tour design.

BACKGROUND

Circular Restricted Three-Body Problem

The primary model used for these analyses is the CRTBP or the planar CRTBP (PCRTBP). A brief description of this model is provided here, and Szebehely[40] may be referred to for more details. In this model, the motion of an infinitesimal mass is modeled in a system containing two massive bodies, referred to here collectively as the primaries, that rotate about their center of mass in circular orbits. The equations of motion

may be written in a rotating frame as

$$\begin{aligned}\ddot{x} - 2\dot{y} &= x - (1-\mu)\frac{x-x_1}{{r_1}^3} - \mu\frac{x-x_2}{{r_2}^3} \\ \ddot{y} + 2\dot{x} &= \left(1 - \frac{(1-\mu)}{{r_1}^3} - \frac{\mu}{{r_2}^3}\right) y \\ \ddot{z} &= -\left(\frac{(1-\mu)}{{r_1}^3} + \frac{\mu}{{r_2}^3}\right) z.\end{aligned} \tag{1}$$

Using this formulation, the x axis in the rotating frame is chosen so that it is aligned with the primaries, and dimensionless quantities are used. The mass of the larger body (the primary) is $1-\mu$, and the smaller body (the secondary) has mass μ. The μ values of several systems used in this analysis and others included for reference are given in Table 1. The primary is then located on the x axis at $x_1 = -\mu$, and the secondary is

Table 1. Mass ratios for selected CRTBP systems

System	μ	System	μ
Sun-Earth	0.0000030404234021	Jupiter-Europa	0.0000252664488504
Sun-Jupiter	0.0009538811803631	Jupiter-Ganymede	0.0000780369094055
Sun-Neptune	0.0000515112366612	Jupiter-Callisto	0.0000566799875169
Earth-Moon	0.0121505842705715	Saturn-Titan	0.0002365805491104
Jupiter-Io	0.0000470509314157	Neptune-Triton	0.0002087756659301

located on the x axis at $x_2 = 1-\mu$. The dimensionless period of the rotating system is 2π, while the distance between the primaries, the mean motion, and the gravitational constant are all one. Finally, the distances from the infinitesimal mass to the primary and secondary are r_1 and r_2, respectively.

An energy-like integral of motion called the Jacobi constant is also known to exist in this problem. It may be computed as

$$C = x^2 + y^2 + \frac{2(1-\mu)}{r_1} + \frac{2\mu}{r_2} - \dot{x}^2 - \dot{y}^2 - \dot{z}^2. \tag{2}$$

It is also known[9] that the Tisserand parameter, which is an approximation of the Jacobi constant, may be written as a function of V_∞ using

$$T = 3 - V_\infty^2. \tag{3}$$

This relationship may be used throughout this work to roughly relate the results at each Jacobi constant to V_∞. For selected Jacobi constants positions exist where the resulting velocity is imaginary. A spacecraft cannot travel into these forbidden regions without a maneuver, and the curve bounding them is referred to as a zero velocity curve.

Five equilibrium points are also found in this problem (the Lagrange points) about which unstable periodic orbits exist. These unstable orbits and other unstable orbits found in the CRTBP are known to possess stable and unstable manifolds. Heuristically, the stable (unstable) manifolds may be thought of as the trajectories that approach the unstable periodic orbit of interest as the time goes toward infinity (negative infinity). More formally, the stable and unstable manifolds for a flow ϕ_t are

Stable Manifold $W^s(L)$: The set of points x such that $\phi_t(x)$ approaches L as $t \to \infty$.

Unstable Manifold $W^u(L)$: The set of points x such that $\phi_t(x)$ approaches L as $t \to -\infty$.

An offset of approximately 1×10^{-6} dimensionless units is used to globalize the invariant manifolds in this analysis.[41] In the Jupiter-Europa system this value corresponds to approximately 0.671 km. See Parker and Chua[42] or Wiggins[43] for more details on invariant manifolds.

For those trajectories computed in the CRTBP a symmetry exists so that departure trajectories can be computed directly from the approach trajectories presented in this work. Specifically, if $(x, y, z, \dot{x}, \dot{y}, \dot{z}, t)$ is a solution in the CRTBP, then $(x, -y, z, -\dot{x}, \dot{y}, -\dot{z}, -t)$ is also a solution.[40,44,45] This symmetry exists precisely in the CRTBP and approximately in the ephemeris model.

Poincaré Sections

Poincaré maps are used throughout this analysis as a means to more easily visualize the relationship of a trajectory to the invariant manifolds of unstable orbits. See Anderson and Lo[20] for a more detailed description of the techniques as they are used here or Wiggins[43] for a more generic explanation. Briefly, they are computed by placing a hypersurface Σ or surface of section in $\mathbb{R}^{n-1}$ transverse to a flow in $\mathbb{R}^n$. The mapping is from one intersection of the trajectory with Σ to the next. For this work it has been found to be most convenient to place Σ on the $y = 0$ line on the opposite side of the primary from the secondary. So for this Poincaré section C is held constant, and $y = 0$. Then given known values for x and $\dot{x}$,

$$\dot{y} = \pm\sqrt{x^2 + y^2 + \frac{2(1-\mu)}{r_1} + \frac{2\mu}{r_2} - \dot{x}^2 - C}. \tag{4}$$

A one-sided Poincaré map is computed here with $\dot{y} > 0$. A Runge-Kutta Fehlberg seventh-order integrator with stepsize control is used to generate the Poincaré sections.

The majority of the Poincaré sections shown here are plotted using x and $\dot{x}$ given that $\dot{y} = 0$. Occasionally it is helpful to plot using the Delaunay variables[12] L and $\bar{g}$. L is the square root of the semimajor axis, and $\bar{g}$ is the argument of periapse relative to the rotating x-axis. A relationship between L and the resonance can be written as

$$\frac{p}{q} = \frac{n_p}{n_q} = \frac{T_q}{T_p} = \frac{\sqrt{\frac{{a_q}^3}{\mu_G}}}{\sqrt{\frac{a_p^3}{\mu_G}}} \approx {a_p}^{-3/2} = L^{-3} \tag{5}$$

where μ_G is the gravitational parameter of the primary.

Single-Shooting Algorithm and Continuation

A single shooting method[46] based on the symmetry about the x-axis in the CRTBP mentioned earlier was used to compute the libration and resonant orbits for this analysis. Some modifications were made to the algorithm to account for the fact that the first intersection with the x-axis is not necessarily the desired intersection for some resonant orbits. The instability of the orbits computed here puts a lower limit on the error of approximately 10^{-11} for the single shooting technique.[47]

Once a periodic orbit in a particular family is computed, a continuation method[46] is used to compute more orbits in the family. A continuation method similar to that used by Gómez, Llibre, Simó 2001[48] was implemented for this study. For this work, the same type of corrector was used, but a simple linear extrapolation[49] was found to be sufficient as a predictor for most of the cases.

RESONANCES REQUIRED FOR APPROACH THROUGH THE LYAPUNOV ORBIT GATEWAY

Given the knowledge that Lyapunov orbits act as a gateway, it is natural to use this gateway as a starting point to search for trajectories approaching a moon or the secondary in the CRTBP. The invariant manifolds of these Lyapunov orbits at a given Jacobi constant divide the phase space and allow us to determine those trajectories with the conditions necessary to approach the region around the secondary. One method to determine the properties of the trajectories with the characteristics required to enter this region is to look at the stable manifolds of the Lyapunov orbit integrated backward in time. A convenient method for easily visualizing these stable manifolds relative to other trajectories is to compute their intersections with Σ. This technique provides a means to assess the resonance required at a point some time prior to final approach. The trajectory is least perturbed by the secondary at this point, and resonant orbit intersections along with invariant manifolds can be computed relative to this Poincaré section to evaluate trajectories capable of approach.

The Lyapunov orbit invariant manifolds could be extended further back in time, but the question of immediate interest in this study is which resonances allow for a relatively direct approach. We want to back up to find the last resonance or one of the last resonances that the trajectory needs to travel through before the final approach. It is possible that the trajectory could travel backward in time through several resonances and one of the resonances could be found, but the last resonance in the sequence is the one of interest for this work. Direct approaches may also be targeted with large ΔVs, but this study focuses on the low-energy regime. The results from this section answer the question of which resonance is necessary for a particular approach by examining variations in both C and μ.

Lyapunov Orbit Characteristics in Selected Systems

The first step in the process of analyzing the resonances enclosed by Lyapunov orbits in various systems is to compute the Lyapunov orbits using continuation over a range of Jacobi constants. The orbits are commonly computed in the literature,[50,51] and their characteristics are well-known. As many of the possible missions of interest involve approaches from exterior resonances, this study focuses on computing L_2 libration orbits.

The range of Jacobi constants used here for each L_2 Lyapunov orbit family are given in Figure 1(a) for the selected set of three-body systems. The range in each of these cases terminates at the lower Jacobi constant where the Lyapunov orbits in the family encounter the surface of the moon. The Lyapunov orbit family can, of course, generally be continued below the surface of the moon, and the dynamics of the associated invariant manifolds may still be used by spacecraft within the system. The upper bound on the Jacobi constant for

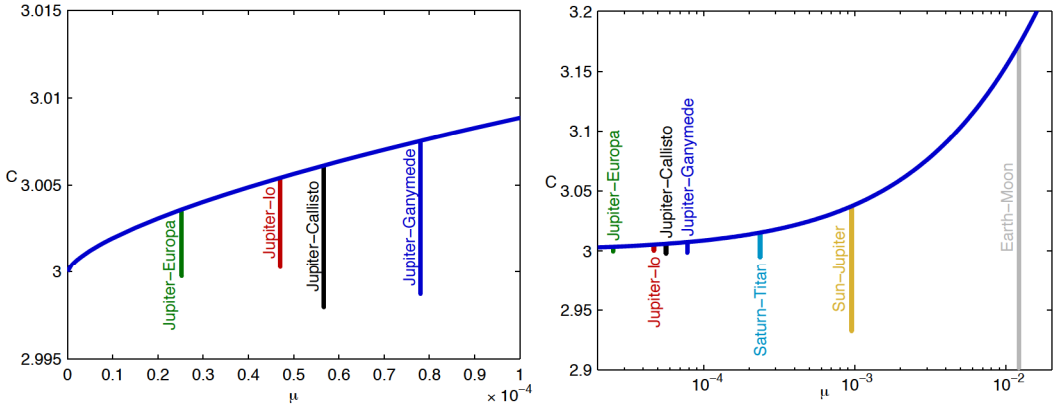

(a) Jovian Moon Systems

(b) Overview of Selected Systems

Figure 1. The ranges of the Jacobi constants of each set of Lyapunov orbits at L_2 considered for each system over different values of μ. The upper bound is the Jacobi constant at the L_2 libration point, and the lower bound is set where the Lyapunov orbit encounters the surface of the secondary. (Note that a log scale is used for the horizontal axis of (b))

each system is given by the Jacobi constant of the libration point, because the Jacobi constants of the orbits approach this value as the orbits become very small.

Possible Approach Resonances for Different Systems (Vary μ)

As a first step in estimating the resonances that are required for approach to the secondary, the resonances enclosed by the Lyapunov orbit stable manifolds may be computed over different Jacobi constants. As the Jacobi constant is decreased, the Lyapunov orbit manifolds stretch to enclose additional resonances. For most mission design applications, having these additional resonances available is a potentially desirable option because the resonances included at lower Jacobi constants deviate the most from a 1:1 resonance with the secondary. Access to these resonances is beneficial since the spacecraft is typically attempting to approach

the secondary from distant resonances. In the following discussion, the term near will be used to refer to those resonances that are closer to a 1:1 resonance with the secondary, and the term distant will be used to refer to those resonances that vary the most from the 1:1 resonance. In the case of Europa orbiter trajectories, the trajectory typically winds down from distant exterior resonances with the goal of coming closer to the 1:1 resonance. Once the trajectory reaches a resonance enclosed by the Lyapunov orbit manifolds it becomes possible to enter through the Lyapunov orbit gateway and approach the secondary. So from this perspective, the fact that the Lyapunov orbit manifolds at lower Jacobi constants enclose the greatest number of resonances including those deviating the most from the 1:1 resonance means that examining the invariant manifolds of these Lyapunov orbits would reveal the resonance required for approach to the secondary using the most direct path as the trajectory traverses the resonances. There are other factors to consider such as how to tie the approach into the rest of the tour and whether a potential ΔV is needed to target the proper energy. But for this first portion of the analysis, the Lyapunov orbit on the low end of the Jacobi constant range in each system corresponding to the Lyapunov orbit that grazes the surface of the secondary was used to obtain an estimate of the typical minimum requirements on the resonances required for approach. For the energies typically found in an endgame scenario,[20,30] this method therefore provides a bound on the resonances required for the approach. It is also worth noting that the Lyapunov orbit families can be computed for those orbits going below the surface of the secondary, so the energy range may be extended this way if so desired. For this study, this condition was selected as a bound, and most traditional endgame scenarios will likely fall in this energy range. At higher Jacobi constants, fewer resonances may be available, but this will be examined later.

The trajectories on the Lyapunov orbit stable and unstable manifolds are computed in each case as given in Figure 2, and the intersections with the surface of section given in the figure are recorded. This process

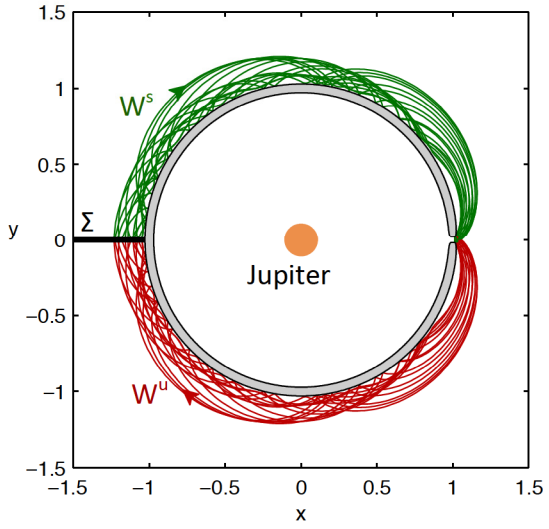

Figure 2. Illustration of the stable and unstable manifolds of an L_2 Lyapunov orbit in the Jupiter-Europa system for C = 3.0025. The trajectories on the invariant manifolds are computed until they reach the selected surface of section, Σ, on the y = 0 line on the far side of Jupiter from Europa.

is repeated for selected systems over a range of Jacobi constants, and the results are shown in Figure 3. In each case the same colors are used to designate the stable and unstable manifolds as used in Figure 2, and the intersections with the $\dot{x} = 0$ line indicate potential enclosures of new unstable resonant orbits as found in Anderson and Lo.[20] In any case, examining the invariant manifolds shows the range of x values reached for these conditions, and consequently the potential targets for approach in terms of approximate resonances. More details on these resonances will be given shortly, but it is enlightening to compare the differences in the various systems. Keep in mind that these systems are different in their μ values as well as the Jacobi constant where the L_2 Lyapunov orbit grazes the surface of the secondary and the scale of x on the horizontal

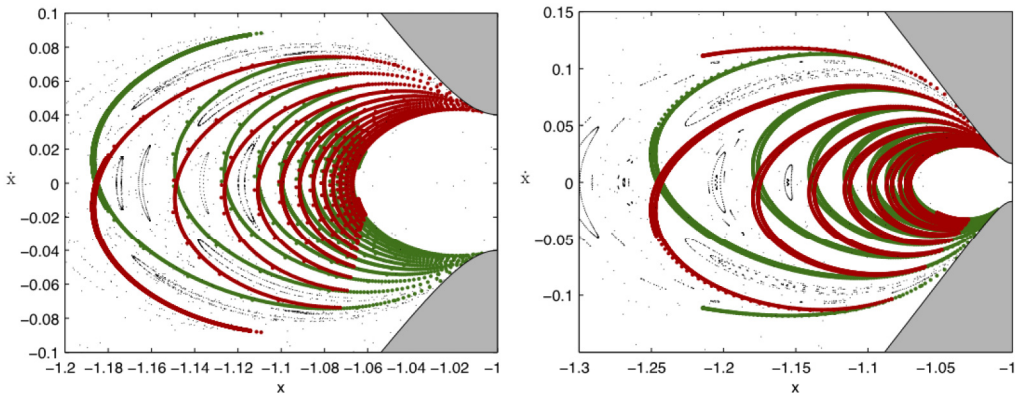

(a) Sun-Earth

(b) Jupiter-Europa

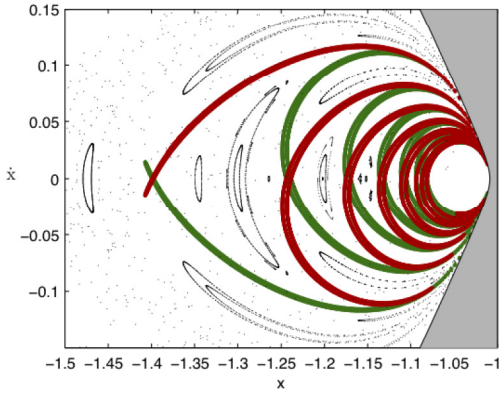

(c) Jupiter-Io

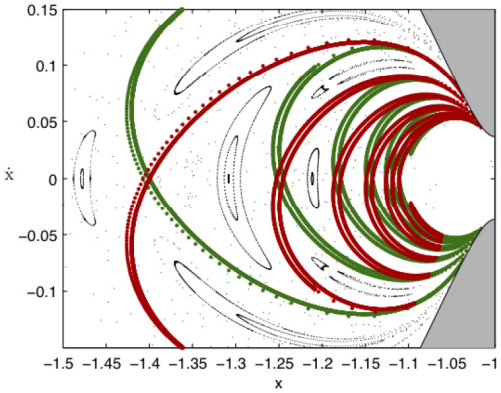

(d) Jupiter-Ganymede

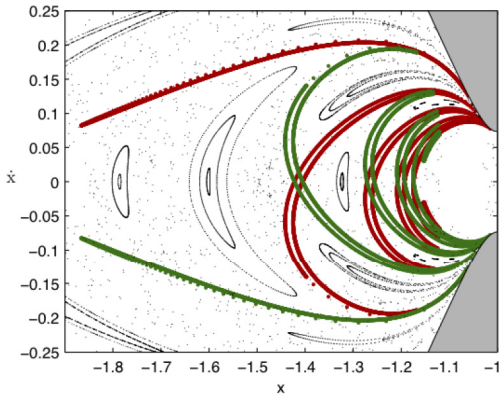

(e) Saturn-Titan

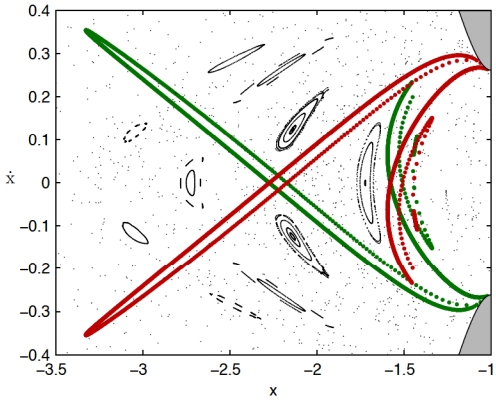

(f) Sun-Jupiter

Figure 3. Poincaré section along Σ showing the intersection of the stable manifold of the L_2 Lyapunov orbit in green and the intersection of the unstable manifold in red. In each case, the plot is given for the Jacobi constant corresponding to a Lyapunov orbit that just grazes the surface of the secondary in the designated system.

axis. Several general trends can be observed though. Noticing that the x-axis scale differs in some of the plots, it can be seen that in general as μ increases, the intersections reach further away from -1. This does

not mean however that a greater number of potential resonances is necessarily enclosed. This trend continues as μ is increased with similar results for the Earth-Moon system. More specifically, it appears that the most distant resonance that is reached in the Jupiter-Europa system is the 5:6 resonance. The arms of the invariant manifolds at the top and bottom of this plot would extend to the left further if the Jacobi constant were decreased more, and it could be imagined that for very high energies, or low Jacobi constants, they might approach the 3:4 resonance. This is the case especially if the arms are not required to reach $\dot{x} = 0$, and an approximate resonance might be targeted. The 5:6 resonance is definitely enclosed for this case, but for the Jupiter-Io and Jupiter-Ganymede systems with slightly higher μ values, it appears that a new resonance is potentially enclosed. The Jupiter-Io system seems to just barely reach this resonance, and the Jupiter-Ganymede system reaches it handily. A similar situation appears to exist for the Saturn-Titan system, but at this point, the manifolds are beginning to travel to another resonance. It can be imagined that a trajectory could target the stable manifold arm by using a nonzero $\dot{x}$ for more negative values of x. Finally, for the Sun-Jupiter system it appears that the arms reach this more negative crossing on the x-axis. A more detailed look at several of these cases will be considered next.

Relationship of Resonant Orbits to Lyapunov Orbit Invariant Manifolds

Up until this point, it has been assumed that when the invariant manifolds of the Lyapunov orbits stretch further to another position on the $\dot{x} = 0$ axis, they are enclosing or reaching the vicinity of new resonant orbits from which a final approach may be planned. The details of the final approach design will depend heavily on the particular resonant orbit that is selected and its relationship to the invariant manifolds of the Lyapunov orbit at the same Jacobi constant. Several resonant orbit families are computed here, and the types of families are compared to determine which ones are most beneficial for use in the final approach.

First, it is helpful to provide a brief definition of resonance as it is used in this paper. Resonant orbits in the two-body problem are defined in a straightforward manner. In this model, a body is periodic in the rotating frame when the body travels around the primary p times for every q times the secondary travels around, where $p, q \in \mathbb{N}$. The relationship between the resonant integers, mean motions, and periods of the spacecraft and the smaller primary may be written as

$$\frac{p}{q} = \frac{n_p}{n_q} = \frac{T_q}{T_p}, \tag{6}$$

respectively. In this paper, the form p:q is used to denote the resonances, which is the same as [secondary period]:[spacecraft period] or [spacecraft revolutions]:[secondary revolutions]. Murray and Dermott[52] may be referred to for a more detailed explanation of resonance in the three-body problem. For this case where the three-body perturbations become important they define resonance according to

$$pn_p \approx qn_q \tag{7}$$

See Anderson and Lo[20] for a more detailed explanation of resonance as it is used here.

Resonant orbits may be computed using a variety of different techniques. The resonant orbits examined in this study are symmetric about the $y = 0$ line such that they lie on the $\dot{x} = 0$ line of the Poincaré section computed using Σ in Figure 2. One method for computation of these resonant orbits is to continue them from approximate two-body orbits with the desired period into the three-body problem with the desired value of μ by gradually increasing μ from near zero or another value where the approximation is considered valid. This technique is commonly used,[6,22] and it is used to compute some of the orbits presented here. For this method, an initial guess for the initial velocity of this resonant orbit with μ near zero may be computed as

$$v_{dim} = \sqrt{2\left(-\frac{GM}{2a_{dim}} + \frac{GM}{x_{0dim}}\right)} \tag{8}$$

where the initial guess is assumed to be on the $y = 0$ line at an apse. The values for velocity (v), semimajor axis (a), and gravitational parameter (GM) are all dimensional. If GM is assumed to be that of the barycenter,

the dimensionless equation can be written simply as

$$v = \sqrt{2\left(-\frac{1}{2a} + \frac{1}{x_0}\right)} \tag{9}$$

The value for a may be determined from the resonance as

$$a = \left(\frac{\mathbb{P}_{s/c}}{\mathbb{P}}\right)^{2/3}. \tag{10}$$

So for a 3:4 exterior resonant orbit, the ratio in the parenthesis would be 4/3. Given this initial position and velocity in the inertial frame, the state may then be transferred to the rotating frame as an initial guess for the resonant orbit. In general, it has been found that this technique provides a good initial guess for the continuation. Another method that is commonly used for computing libration point orbits, using the analytical expansions around the libration points,[53] is not available here, so a numerical search along a grid of initial conditions is made use of to compute several of the desired resonant orbits. For these cases, a grid computing trajectories in parallel is sometimes used to speed up the process. By virtue of the algorithm used to compute them, the resonant orbits at each resonance, at least those computed in this work, are located on the $\dot{x} = 0$ line in the Poincaré sections. So each new intersection of the Lyapunov orbit manifolds with this line as the Jacobi constant decreases represents the enclosure of a potential new resonance or resonant orbit. Again, this is not to say that a trajectory with a small value of $\dot{x}$ could not be used to target the gateway.

It has been mentioned that several different families of orbits may exist near a particular resonance. They often have similar but not exactly the same periods, and they are topologically different. In previous work several different types of resonant orbits have been found to exist near a particular resonance.[27] One resonant orbit was found in particular that came from the exterior region, passed by Europa between Europa and Jupiter, and then returned to the exterior region. This 5:6 resonant orbit was found to lie entirely within the invariant manifolds of the L_2 Lyapunov orbit at this energy level which corresponded to a final approach of the PEO. Other families of unstable resonant orbits exist for this resonance and for different energy levels, so it is worth comparing these orbits to determine their relationship to the invariant manifolds of Lyapunov orbits. It is also worth determining whether the relationship discovered earlier holds true for different Jacobi constants.

As an initial examination of this problem, the 5:6 orbit in the Jupiter-Europa system is computed for different energy levels, and a comparison is made to another resonant orbit at the 5:6 resonance. This family was computed here for a wider range that includes the energy where the Lyapunov orbit grazes the surface of Europa, and the resulting orbits are plotted in Figure 4(a). A 5:6 resonant orbit family computed using continuation from a two-body initial guess is given in Figure 4(b). It can easily be seen that the families pass on different sides of Europa at their close approaches. The family in Figure 4(a) will be referred to as the 5:6-NI family for a 5:6 resonant orbit with no loop on the line of syzygy that passes through the interior, and the family in Figure 4(b) with one loop on the line of syzygy near Europa on the outer region will be designated as a 5:6-LO orbit. One interesting feature of the 5:6-NI orbits is that some of them develop loops on either side of Europa, but they only exist for certain energies. The family may be further continued as the neck region to the right of Europa moves down to the $y = 0$ line and crosses it, but these orbits are not needed here.

To answer one of the initial questions of this study as to whether the 5:6 orbit examined previously stays within the Lyapunov orbit invariant manifolds for different Jacobi constants and how this compares to other 5:6 orbits, each type of 5:6 orbit was computed for the Jacobi constant where the Lyapunov orbit grazes the surface of Europa. Their intersections with Σ compared to the Lyapunov orbit invariant manifolds are shown in Figure 5. The resonant orbits at this energy are similar to the resonant orbits at the lowest energies shown in Figure 4. The intersections show that the 5:6-NI orbit lies within the stable manifold of the Lyapunov orbit while the 5:6-LO orbit falls outside of them. This result might be expected since the 5:6-NI orbit has to pass through the L_2 gateway while the 5:6-LO orbit does not. This fact does have implications for the final approach. It indicates that the 5:6-NI orbit may be the more obvious choice to start from if a close approach to

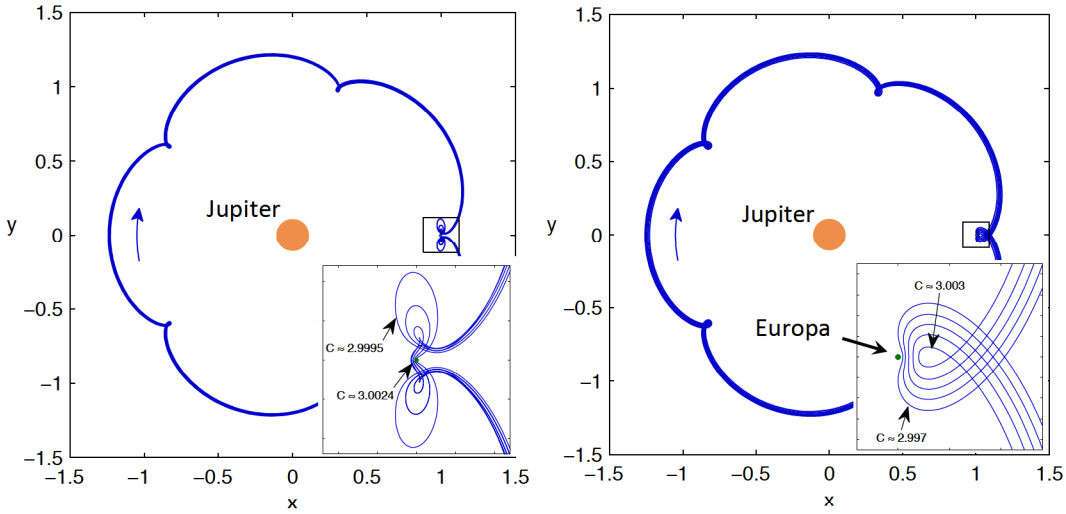

(a) Family with a passage between Jupiter and Europa, 5:6-NI (b) Family with a passage on the far side of Europa, 5:6-LO

Figure 4. Two 5:6 resonant orbit families in the Jupiter-Europa system

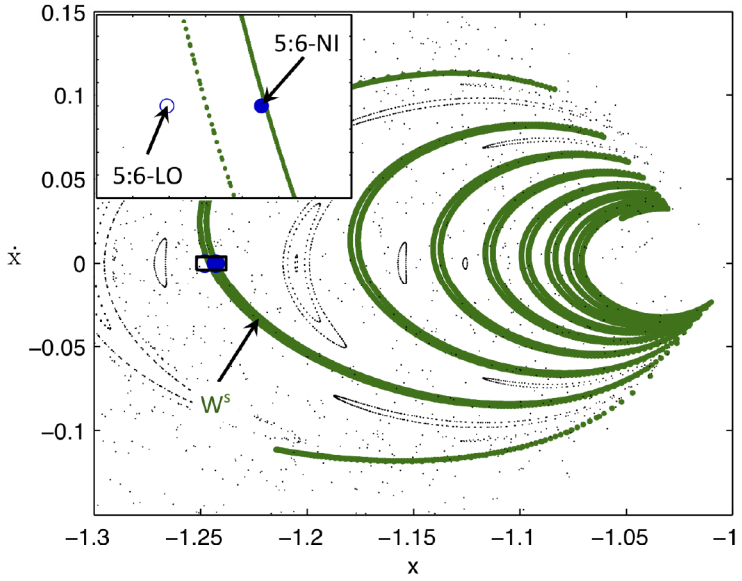

Figure 5. Poincaré section along Σ showing the intersection of the stable manifold of the L_2 Lyapunov orbit in green. Plotted for the Jacobi constant where the L_2 Lyapunov orbit just grazes the surface of Europa. (C = 2.9997485449927250)

Europa is desired. Indeed, at this energy, the 5:6 inner resonant orbit directly encounters Europa. Of course its invariant manifolds also encounter Europa, and some of the invariant manifold trajectories also travel even closer to the center of Europa, which is important for other energies and systems where the resonant orbit travels above the surface of the desired body. The outer resonant orbit remains far from Europa, and its invariant manifolds do not travel to Europa over the time periods of interest here. The analysis so far has confirmed the existence of these different types of resonant orbits over different energies in the Jupiter-Europa system for the 5:6 resonance. The location of the 5:6-NI orbit within the stable manifold of the Lyapunov orbit indicates that it is a potentially desirable type of orbit. A further question is do these types of orbits

exist in other systems and for other resonances where they might be useful for approach? This ties in with the previous analysis in determining the minimum requirements on the resonance for the final approach phase.

The next case chosen for analysis to explore this question is the Jupiter-Ganymede system. In this system, the invariant manifolds of the Lyapunov orbit appear to just reach the 3:5 resonance. So in this case the approach for different resonance, μ, and C values is examined. For this case, a numerical search was conducted with a grid to look for an orbit with characteristics similar to the Jupiter-Europa 5:6-NI orbit with these new criteria in mind. The resulting family of orbits is given in Figure 6(a). The family shown here was

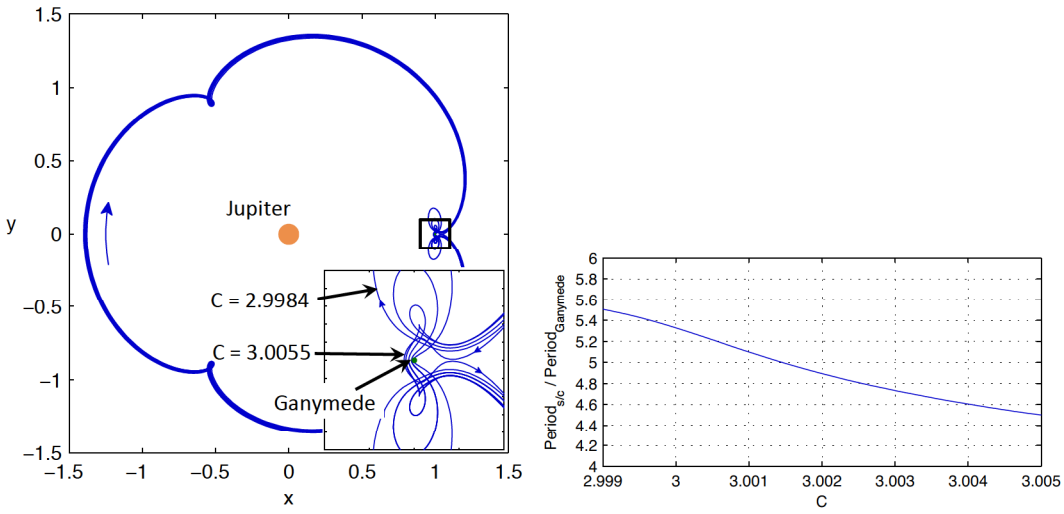

(a) View of the family in the xy plane

(b) Periods of the family of orbits

Figure 6. The Jupiter-Ganymede 3:5 resonant orbit family with the corresponding orbit periods.

continued a little further than for the Jupiter-Europa case, but the Jupiter-Ganymede case at this resonance has the same general characteristics as those seen in the Jupiter-Europa case. Now the question of the resonance that the Lyapunov invariant manifolds are reaching on the far left of the Poincaré sections can be more precisely answered. From the plots of the family in position space, it can be seen that there are three major loops on the trajectory as it travels around Jupiter. Each of these loops corresponds to a periapse, indicating that three revolutions of the spacecraft have occurred. The number of revolutions of the secondary in this time period can be computed by looking at the period of the orbit relative to the period of the secondary. The periods normalized by the period of Ganymede for the resonant orbit family computed in Figure 6(a) are given as a function of C in Figure 6(b). It can be seen that the period actually varies noticeably depending on the value of C. This is where the difference between resonance in the two-body and three-body problems becomes apparent, as the relationship of the periods is approximate in the three-body problem. It does appear that especially for the Jacobi constants typically of interest for mission design, the trajectory is near the 3:5 resonance.

Now, if the trajectory's intersection with the surface of section is shown relative to the stable manifold of the Lyapunov orbit as given in Figure 7, it can be seen that this orbit lies within the manifold as well. From this result it appears that this type of orbit exists at least for a significant subset of possible cases, and if this type of orbit allows for easier approaches in the final phase of the endgame, it is an important type of orbit to consider in the design process. The utility of this type of orbit will be examined relative to approaches using the invariant manifolds of the Lyapunov orbits in a later section.

Possible Approach Resonances for Different Jacobi Constants (Vary C)

Now that the most distant resonances generally feasible for approach for each system have been shown, one question, especially for a trajectory approaching from exterior resonances might be at what Jacobi constant

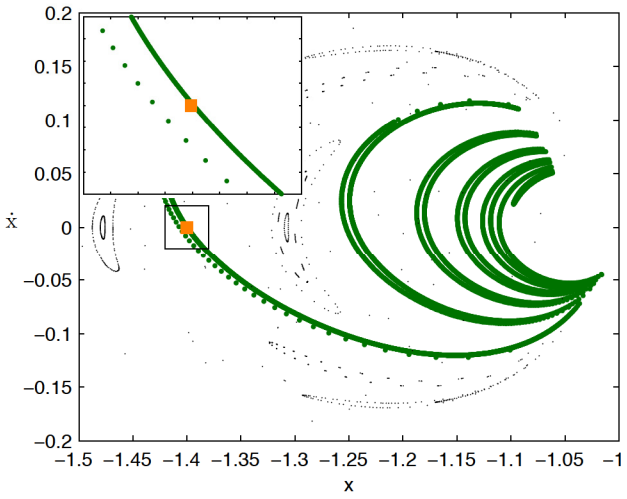

Figure 7. Poincaré section at Σ showing the intersection of the stable manifold of the L_2 Lyapunov orbit in green. Plotted for the Jacobi constant where the L_2 Lyapunov orbit just grazes the surface of Ganymede. (C = 2.99872421138553)

levels are the resonances available? This question must be considered in combination with the ΔV for capture which would decrease with higher Jacobi constants or lower energy. Another question is what is the lowest Jacobi constant that a particular resonance would be feasible to use for approach when the resonant orbit is enclosed in the resonance? An initial look at four sample energies in Anderson and Lo[37] showed some evolution in the Lyapunov invariant manifolds with energy that indicated some resonances might no longer be enclosed as C increases. This possibility is examined in more detail here using the Saturn-Titan system as an example. The Poincaré sections including the invariant manifolds of the Lyapunov orbit are shown for several Jacobi constants in Figure 8. It can be seen from this series that as the Jacobi constant increases, fewer resonances are enclosed. Above C $\approx$ 3.0148 the invariant manifolds no longer encounter the $x = 0$ line, and as C increases further, the invariant manifold intersections move further from this line. So at this point, the L_2 gateway would require a nonzero $\dot{x}$ to target the final approach.

A similar situation exists for the other systems analyzed here, and the Poincaré sections for several selected cases for the C where the Lyapunov orbit invariant manifolds start to fall away from the most distant resonance are shown in Figure 9. One interesting feature seen in these plots is that the closer resonances tend to leave the Lyapunov invariant manifold enclosure first. The outer resonances seen in Figure 3 tend to stay available longer until the Jacobi constants labeled in each subfigure. Even so, it can be seen that in some of the figures, a small value of $\dot{x}$ would allow the gateway to be targeted for even higher values of C. Another interesting result is the different behavior in the Saturn-Titan case. The invariant manifold arms stretching to the left in this case did not quite reach the $\dot{x} = 0$ line, and as the Jacobi constant increases the stable manifold covers the most distant resonance until the Jacobi constant becomes relatively high.

ORBIT INSERTION VIA LYAPUNOV AND RESONANT ORBIT INVARIANT MANIFOLDS

The desirability of different approaches to Europa may be measured using several different metrics. Of course the desired characteristics will depend on the overall purpose of the mission, such as whether the spacecraft is a lander or orbiter, and constraints imposed at the beginning of the final approach phase must be taken into account. One metric that can be used for an orbiter mission is the ΔV required to insert into a circular orbit around the secondary. The approach trajectories using the invariant manifolds of resonant orbits are analyzed here and compared to the approaches possible using Lyapunov orbit invariant manifolds at the same energies. This type of trajectory was investigated previously for a single case.[54] An invariant manifold trajectory of a resonant orbit was also found to eventually approach the vicinity of the secondary

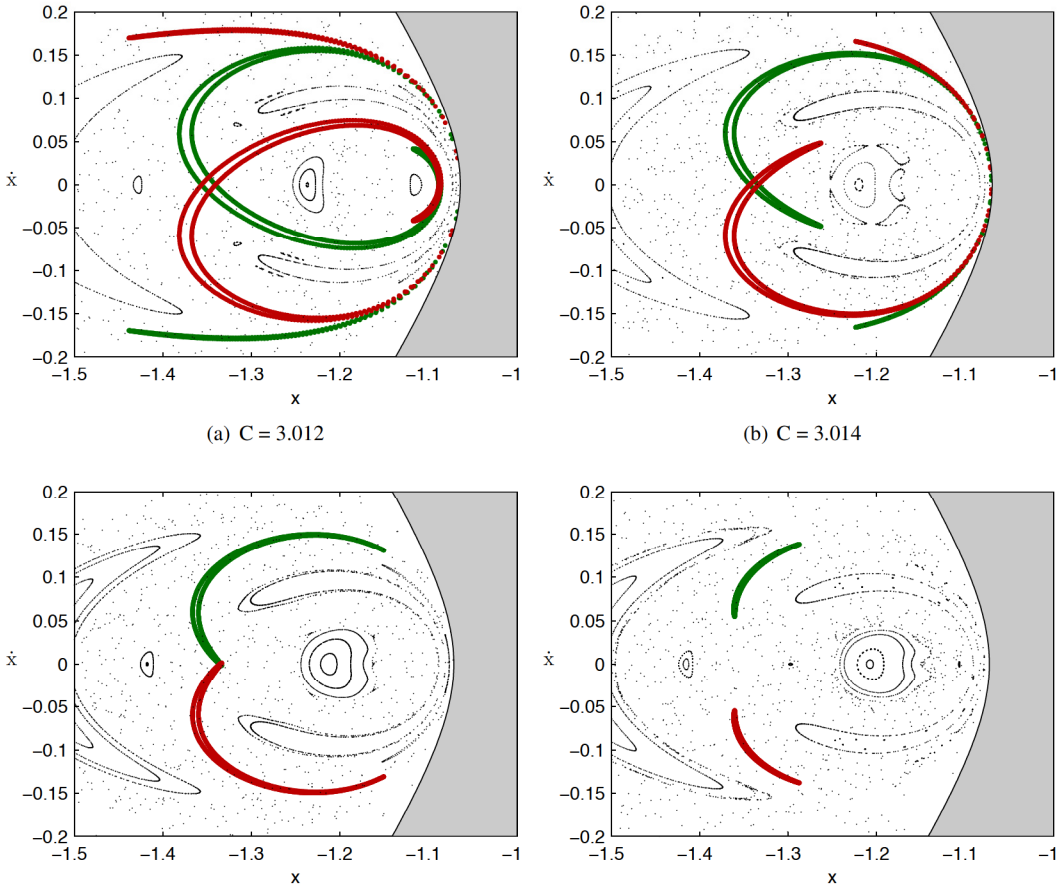

(a) C = 3.012 (b) C = 3.014

(c) C = 3.014780 (d) C = 3.0153

Figure 8. Poincaré sections showing the stable and unstable manifolds of the L_2 Lyapunov orbit for different Jacobi constants in the Saturn-Titan system.

after a significant period of time in Vaquero and Howell.[22] Here we are more interested in trajectories that approach the secondary from the resonant orbit more directly. It is expected that the ΔV will be minimized by searching for the invariant manifold trajectories that possess a periapse at the desired altitude of 200 km. In each case, the trajectory is assumed to be inserted into an orbit with a velocity in the same direction as the approach trajectory. Assuming that these orbits insert tangentially, it is expected that the ΔVs for the Lyapunov orbit and resonant orbit manifolds will be similar. For a given Jacobi constant, the velocity magnitude at a selected position will be defined. So a trajectory on the invariant manifold of a Lyapunov orbit and a resonant orbit at the same Jacobi constant encountering Europa at the same position would have the same velocity magnitude in the rotating frame. The only potential difference is in the velocity direction, and if this is constrained to be tangential, the velocity at this point is the same excepting a possible sign difference. This situation leaves possible differences as a result of the position of the periapse around Europa which does result in some variation in the velocity depending on the system under consideration and the size of the secondary.

For this analysis the unstable manifold trajectories possessing a periapse at 200 km were first computed for the Lyapunov orbits across a selected range of Jacobi constants in each system to verify that they exist at the desired energy and to numerically determine the ΔV required for insertion into a circular orbit. If multiple apses were found, the one possessing the minimum ΔV was selected and saved for comparison with the approach via the resonant orbit unstable manifold. A similar procedure was followed for the resonant orbit,

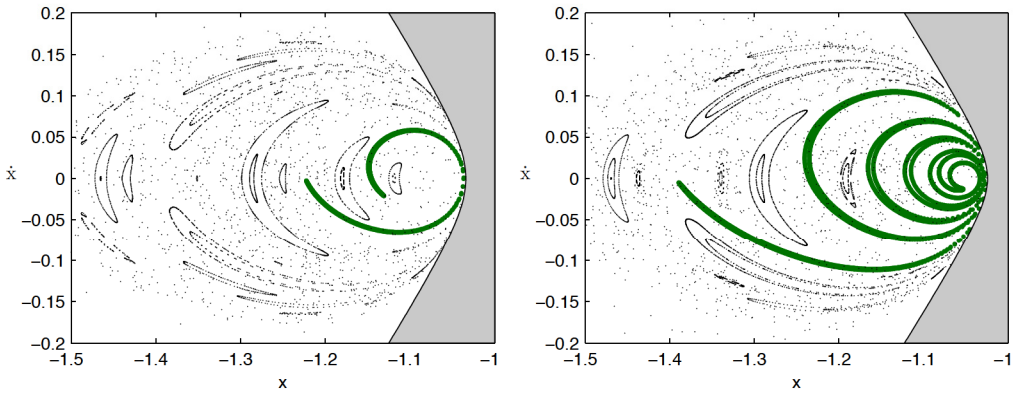

(a) Jupiter-Europa, C = 3.0034

(b) Jupiter-Io, C = 3.0018

(c) Jupiter-Ganymede, C = 3.0066

(d) Saturn-Titan, C = 3.0148

Figure 9. Poincaré sections showing the L_2 Lyapunov orbit stable manifold at C values near the point at which it no longer reaches the $\dot{x} = 0$ line for the distant resonance.

but in this case particular energies were used to verify that approximately the same result could be achieved. The results are plotted in Figure 10 for several different systems. In each case, the color of the line indicates the system that was used, and the solid line corresponds to the Lyapunov orbit results. The points plotted on each line are the results from the resonant orbits. The orbits can often be continued further, but this provides a sample of the results.

The specific characteristics of the approach trajectories originating at the resonant orbit as computed in Figure 4(a) are of interest. One typical trajectory for a Jacobi constant of 3.0024 with a periapse at 200 km is shown in Figure 11. It can be seen that this particular trajectory on the unstable manifold of the 5:6 orbit is integrated from a point just prior to the first Europa flyby. On the second flyby it comes close enough to Europa for the desired orbit insertion. The integration time from the initial offset on the 5:6 orbit is approximately 41.6 in dimensionless units or 23.5 days. It is interesting that the characteristics of this approach trajectory are very similar to the approach of the PEO trajectory analyzed in Anderson and Lo.[20] In analyzing this trajectory keep in mind that it may be possible to target the invariant manifold trajectory at some point after this initial time, such as apoapse on the far side of Jupiter from Europa, to cut out some of the time required for the trajectory. This method was used successfully to develop resonant orbit sequences in Anderson and Lo.[21] For this case the time from this apoapse to orbit insertion was approximately 20.38 dimensionless time units or 11.5 days.

An unstable manifold of the Lyapunov orbit that approaches Europa with a periapse at 200 km is shown in

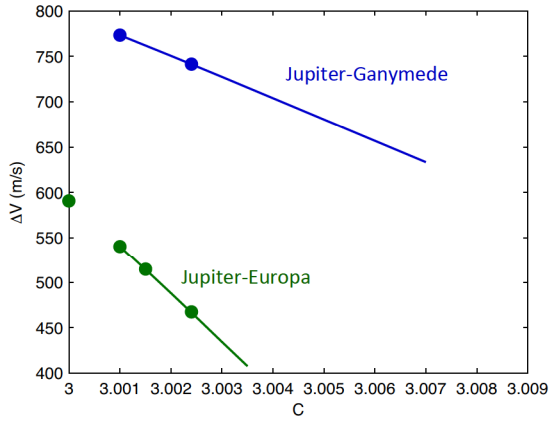

Figure 10. Plots of ΔV to insert into 200 km circular orbits from Lyapunov orbits and resonant orbits over different Jacobi constants in various systems.

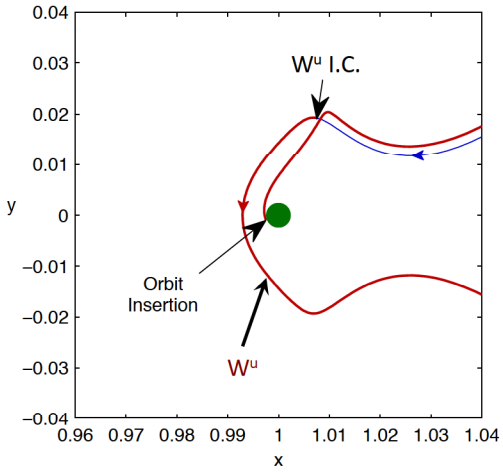

Figure 11. Trajectory on $W^u_{5:6}$ in the Jupiter-Europa system that has a 200 km periapse at Europa. Insertion into a circular orbit from this point requires a ΔV of approximately 467.4 m/s. For these trajectories, C = 3.0024.

Figure 12. For this case, the time of flight of the approach from the Lyapunov orbit to Europa is approximately 4.9 dimensionless units or approximately 2.8 days. The time for approach from the apoapse of the Lyapunov orbit's unstable manifold on the far side of Jupiter may vary depending on the specific trajectory that is selected, but it is typically on the order of 23-24 dimensionless units (13.0-13.6 days) for a trajectory traveling from near the 5:6 resonant orbit. In general there may also be some time involved in connecting these stable and unstable manifold trajectories as the spacecraft travels along the Lyapunov orbit. So the quickest potential transfer from the apoapse opposite Europa via Lyapunov invariant manifolds is on the order of 16 days not including any time for phasing around the manifolds. As might be expected, the resonant orbit's unstable manifold gives a more direct approach to the secondary.

COMPARISON OF MANIFOLDS TO TRAJECTORIES COMING OFF SURFACE

While the invariant manifolds of resonant orbits and Lyapunov orbits provide two options for traveling to the secondary, another tactic for analyzing this approach phase is to integrate trajectories that terminate at the secondary backward in time to eventually connect them to some desired point. This method is used here following the techniques described in Anderson and Parker,[55] and it is similar to the approach taken

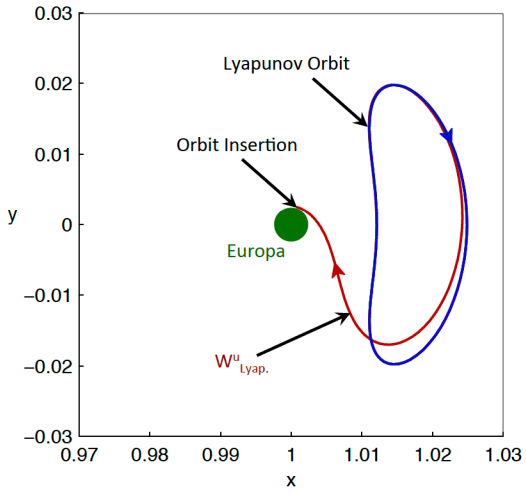

Figure 12. Trajectory on $W^u_{Lyap.}$ in the Jupiter-Europa system that has a a 200 km periapse at Europa. Insertion into a circular orbit from this point requires a ΔV of approximately 466.5 m/s. For these trajectories C = 3.0024.

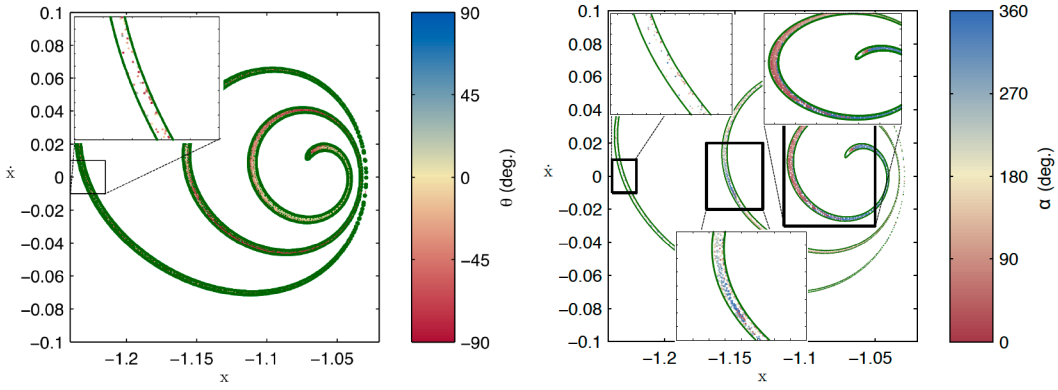

(a) Plot showing θ (b) Plot showing α

Figure 13. Poincaré section at Σ showing the intersection of the stable manifold of the L_2 Lyapunov orbit in green. θ values of 0^o correspond to an impact normal to the surface at Europa. (Plotted for C $\approx$ 3.0025.)

by Grebow et al.[32] that was mentioned previously. In this case, however, the focus is on shorter time spans for the last segment of the trajectory. The previous works typically focused on larger time intervals. In this case a comparison is made to the invariant manifolds of the Lyapunov orbit to determine the nature by which target points for specific types of trajectories to the surface may be selected. Some interesting questions to be answered are related to whether trajectories with particular approach parameters are grouped together within the stable manifold and how the enveloping stable manifold may be used as a guide or boundary for mission design. The method used here is applicable to landing trajectories, which are currently of some interest, traveling to the surface of the secondary. It should be mentioned that this technique can be easily applied to orbit insertion using trajectories originating above the surface of Europa, and the previous analysis using invariant manifolds for orbit insertion could likewise be extended to landing trajectories. In brief, trajectories are integrated backward in time from the surface of the secondary, which in this case is Europa. The location of the end point of the trajectory is specified by the angle α which is defined to be zero in the positive x direction and is positive in the counterclockwise direction. The velocity coming into the surface is specified

by the angle θ. θ is zero for velocities normal to the surface and positive in the counterclockwise direction as well.

The results for a sample analysis at a Jacobi constant of 3.0025 are shown in Figures 13 and 13(b). The results in Figure 13 plot the trajectories showing the termination angle relative to the surface, and the results in Figure 13(b) plot them relative to the termination position on the surface. As expected, the trajectories approaching the surface of Europa are contained within the invariant manifolds of the Lyapunov orbit. Examining the close-up view in Figure 13, it is interesting that a range of angles relative to the surface seem to be available if the target point in the Poincaré section is changed a little in either x or $\dot{x}$ for most locations. The trajectories in the band seem to be well-mixed with respect to θ. The results plotted relative to the location on the surface seem to be less mixed together. Particular bands of trajectories from specific final destinations are found here, however at each resonant loop, there appear to be a mix of possible targets. These results answer some of the initial questions posed earlier in a general sense. More work has been done to examine this problem for different systems and will be presented in a future paper. The results here provide some additional insights though that are discussed in the next section.

EPHEMERIS EFFECTS

One problem that has been of interest is to gain a more thorough understanding of how the invariant manifolds of unstable orbits deform as the problem is moved from simpler models to more complex. The fact that the trajectories in Figures 13 and 13(b) are enclosed by the Lyapunov manifolds yet seem to fill them out suggests one method that might be used to understand how Lyapunov manifolds change in the ephemeris problem compared to the CRTBP. Rather than attempting to compute the manifolds directly, the trajectories may be integrated from the surface of the secondary as in the CRTBP, and the deviation of this set of trajectories from those in the CRTBP computed with the same velocity profile (Jacobi constant) may be observed. This method also provides a more direct analysis of the trajectories that are often of the most interest, those trajectories that approach the surface or near the secondary. All of the trajectories observed in this case also have a known velocity at the secondary.

A short analysis of these types of trajectories is presented next. Several additional complicating factors are introduced at this point. For trajectories in the ephemeris problem, the initial epoch of the integration becomes important. Additionally, the results will vary over the orbit of the secondary typically varying most widely from periapse to apoapse.[55] An analysis of this variation for trajectories integrated over a 50 day time period and terminating at Europa in the Jupiter-Europa system at two sample epochs is given in Figure 14. Note that for this case, since the problem is no longer in the CRTBP, the complete state may no longer

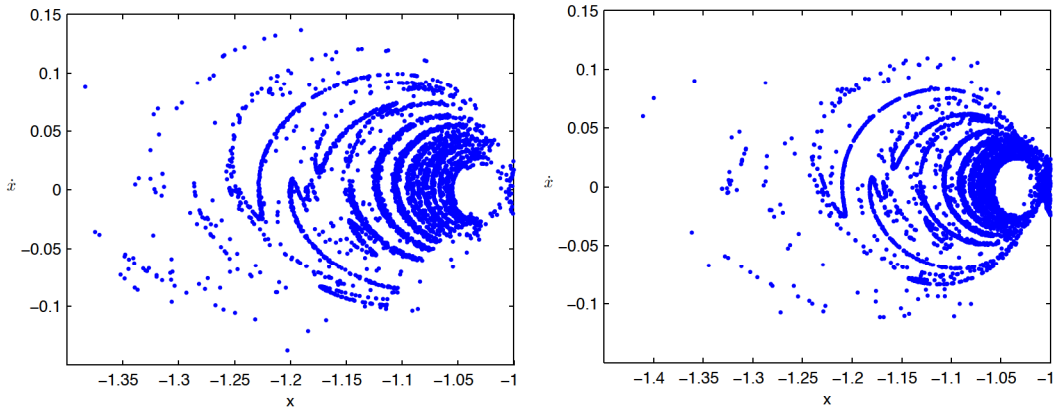

(a) Periapse case

(b) Apoapse case

Figure 14. Intersections with Σ in the ephemeris model of trajectories terminating at the surface of Europa in the Jupiter-Europa system.

be computed from the location of the intersection with Σ. A rough idea of the effects of the ephemeris, however, may still be obtained, especially relative to different dates along the orbit. The results shown here are computed at the periapse and apoapse of Europa, and they show two of the extremes in the distances to which the trajectories travel. It appears that the apoapse case has trajectories that travel further away than the periapse case. If other dates are examined, dates just before and after periapse appear to have trajectories that also travel further away. These initial results indicate that specific trajectories in the ephemeris problems may have desirable qualities for the approach phase, and this avenue will be explored further in the future.

CONCLUSIONS

The resonances required for the final approach in the endgame problem were evaluated for several selected systems using the computation of the invariant manifolds of Lyapunov orbits in the CRTBP. Specific 5:6 and 3:5 resonant orbits were computed for the Jupiter-Europa and Jupiter-Ganymede systems, respectively. A special type of resonant orbit was found to exist for the desired resonance in the Jupiter-Ganymede system as well as in the Jupiter-Europa system, and they were evaluated to determine their suitability for the final approach. These particular orbits were found to be desirable for the approach having ΔVs similar to the Lyapunov orbit case and possessing time of flights roughly 4.5 days shorter than the Lyapunov orbit invariant manifolds. The final approach of a trajectory on the invariant manifold of one of the resonant orbits was found to be similar to the final approach of the planar Europa Orbiter computed in earlier works. The Jacobi constants at which distant resonances were no longer enclosed in the Lyapunov orbit invariant manifolds were quantified and compared for different systems. A comparison of Lyapunov invariant manifolds to trajectories encountering the secondary across its surface showed that they bound these trajectories, and that many potential different approaches are available at each resonance. The fact that the stable manifolds bounded these trajectories was used to take an initial look at the potential change in the invariant manifolds in the ephemeris problem.

FUTURE WORK

Avenues for future work include examining additional systems, including interior resonances, tying the approach into the tour, and adding low thrust to the scenario. These studies are currently in process, and additional work is being done to understand the results within the ephemeris.

ACKNOWLEDGEMENTS

The author would like to thank Martin Lo for his support and helpful discussions on this topic. He would also like to thank Jon Sims and Anastassios Petropoulos for their helpful comments and reviews of this paper. The research presented here has been carried out at the Jet Propulsion Laboratory, California Institute of Technology, under a contract with the National Aeronautics and Space Administration. Funding for this research came from AMMOS/MGSS under the "Tour and Endgame Design using Invariant Manifolds" study.

REFERENCES

[1] J. A. Sims and J. M. Longuski, "Analysis of V_∞ Leveraging for Interplanetary Missions," *AIAA/AAS Astrodynamics Conference*, No. AIAA-1994-3769, Scottsdale, Arizona, August 1-3 1994.

[2] S. Campagnola and R. Russell, "Endgame Problem Part 1: V-Infinity-Leveraging Technique and the Leveraging Graph," *Journal of Guidance, Control, and Dynamics*, Vol. 33, No. 2, 2010, pp. 463–475.

[3] R. C. Woolley and D. J. Scheeres, "Hyperbolic Periodic Orbits in the Three-Body Problem and their Application to Orbital Capture," *AAS George H. Born Symposium*, Boulder, Colorado, May 13-14 2010.

[4] G. J. Whiffen, "Mystic: Implementation of the Static Dynamic Optimal Control Algorithm for High Fidelity Low Thrust Trajectory Design," *AIAA/AAS Astrodynamics Specialists Conference*, No. AIAA-2006-6741, Keystone, Colorado, August 21-24 2006.

[5] G. J. Whiffen and T. Lam, "The Jupiter Icy Moons Orbiter Reference Trajectory," *AAS/AIAA Space-Flight Mechanics Meeting*, No. AAS 06-186, Tampa, Florida, January 22-26 2006.

[6] G. Lantoine, R. P. Russell, and S. Campagnola, "Optimization of Low-Energy Resonant Hopping Transfer Between Planetary Moons," *60th International Astronautical Congress*, No. IAC-09.C1.1.1, Deajeon, Korea, October 12-16 2010.

[7] M. Okutsu, T. J. Debban, and J. M. Longuski, "Tour Design Strategies for the Europa Orbiter Mission," *Advances in the Astronautical Sciences, Astrodynamics* (D. B. Spencer, C. C. Seybold, A. K. Misra, and R. J. Lisowski, eds.), Vol. 109, Part III, San Diego, California, American Astronautical Society, Univelt Inc., 2001, pp. 2269 – 2284.

[8] N. J. Strange and J. M. Longuski, "Graphical Method for Gravity-Assist Trajectory Design," *Journal of Spacecraft and Rockets*, Vol. 39, January-February 2002, pp. 9–16.

[9] S. Campagnola and R. Russell, "Endgame Problem Part 2: Multibody Technique and the Tisserand-Poincare Graph," *Journal of Guidance, Control, and Dynamics*, Vol. 33, No. 2, 2010, pp. 476–486.

[10] K. W. Kloster, A. E. Petropoulos, and J. M. Longuski, "Europa Orbiter Tour Design with Io Gravity Assists," *Acta Astronautica*, Vol. 68, 2010, pp. 931–946.

[11] S. D. Ross and D. J. Scheeres, "Multiple Gravity Assists, Capture, and Escape in the Restricted Three-Body Problem," *Siam Journal On Applied Dynamical Systems*, Vol. 6, 2007, pp. 576–596.

[12] W. S. Koon, M. W. Lo, J. E. Marsden, and S. D. Ross, "Heteroclinic Connections between Periodic Orbits and Resonance Transitions in Celestial Mechanics," *Chaos*, Vol. 10, June 2000, pp. 427–469.

[13] W. S. Koon, M. W. Lo, J. E. Marsden, and S. D. Ross, "Resonance and Capture of Jupiter Comets," *Celestial Mechanics and Dynamical Astronomy*, Vol. 81, No. 1-2, 2001, pp. 27–38.

[14] K. C. Howell, B. Marchand, and M. W. Lo, "Temporary Satellite Capture of Short-Period Jupiter Family Comets from the Perspective of Dynamical Systems," *The Journal of the Astronautical Sciences*, Vol. 49, October-December 2001, pp. 539–557.

[15] M. W. Lo, R. L. Anderson, G. Whiffen, and L. Romans, "The Role of Invariant Manifolds in Low Thrust Trajectory Design (Part I)," *AAS/AIAA Spaceflight Dynamics Conference*, No. Paper AAS 04-288, Maui, Hawaii, February 8-12 2004.

[16] R. L. Anderson and M. W. Lo, "The Role of Invariant Manifolds in Low Thrust Trajectory Design (Part II)," *AIAA/AAS Astrodynamics Specialist Conference*, No. Paper AIAA 2004-5305, Providence, Rhode Island, August 16-19 2004.

[17] R. L. Anderson, *Low Thrust Trajectory Design for Resonant Flybys and Captures Using Invariant Manifolds*. PhD thesis, University of Colorado at Boulder, http://ccar.colorado.edu/~rla/papers/andersonphd.pdf, 2005.

[18] M. W. Lo, R. L. Anderson, T. Lam, and G. Whiffen, "The Role of Invariant Manifolds in Low Thrust Trajectory Design (Part III)," *AAS/AIAA Astrodynamics Specialist Conference*, No. Paper AAS 06-190, Tampa, Florida, January 22-26 2006.

[19] R. L. Anderson and M. W. Lo, "Role of Invariant Manifolds in Low-Thrust Trajectory Design," *Journal of Guidance, Control, and Dynamics*, Vol. 32, November-December 2009, pp. 1921–1930.

[20] R. L. Anderson and M. W. Lo, "Dynamical Systems Analysis of Planetary Flybys and Approach: Planar Europa Orbiter," *Journal of Guidance, Control, and Dynamics*, Vol. 33, November-December 2010, pp. 1899–1912.

[21] R. L. Anderson and M. W. Lo, "Flyby Design using Heteroclinic and Homoclinic Connections of Unstable Resonant Orbits," *21st AAS/AIAA Space Flight Mechanics Meeting*, No. AAS 11-125, New Orleans, Louisiana, February 13-17 2011.

[22] M. Vaquero and K. C. Howell, "Poincaré Maps and Resonant Orbits in the Circular Restricted Three-Body Problem," *AAS/AIAA Astrodynamics Specialist Conference*, No. AAS 11-428, Girdwood, Alaska, July 31 - August 4 2011.

[23] E. Bollt and J. D. Meiss, "Targeting Chaotic Orbits to the Moon through Recurrence," *Physics Letters A*, Vol. 204, August 28 1995, pp. 373–378.

[24] C. G. Schroer and E. Ott, "Targeting in Hamiltonian Systems that have Mixed Regular/Chaotic Phase Spaces," *Chaos*, Vol. 7, December 1997, pp. 512–519.

[25] E. Belbruno and B. Marsden, "Resonance Hopping in Comets," *Astronomical Journal*, Vol. 113, No. 4, 1997, pp. 1433–1444.

[26] M. Lo and S. Ross, "Low Energy Interplanetary Transfers Using Invariant Manifolds of L1, L2, and Halo Orbits," *AAS/AIAA Space Flight Mechanics Meeting*, No. AAS 98-136, Monterey, California, February 9-11 1998.

[27] R. L. Anderson and M. W. Lo, "A Dynamical Systems Analysis of Planetary Flybys and Approach: Ballistic Case," *The Journal of the Astronautical Sciences*, Vol. 58, April-June 2011, pp. 167–194.

[28] G. Lantoine and R. P. Russell, "Near-Ballistic Halo-to-Halo Transfers Between Planetary Moons," *AAS George H. Born Astrodynamics Symposium*, Boulder, CO, May 13-14 2010.

[29] T. Sweetser, R. Maddock, J. Johannesen, J. Bell, P. Penzo, A. Wolf, S. Williams, S. Matousek, and S. Weinstein, "Trajectory Design for a Europa Orbiter Mission: A Plethora of Astrodynamic Challenges," *Advances in the Astronautical Sciences, Spaceflight Mechanics* (K. C. Howell, D. A. Cicci, J. E. Cochran, Jr., and T. S. Kelso, eds.), Vol. 95, Part II, San Diego, California, American Astronautical Society, Univelt Inc., 1997, pp. 901–920.

[30] J. R. Johannesen and L. A. D'Amario, "Europa Orbiter Mission Trajectory Design," *AAS/AIAA Astrodynamics Specialist Conference*, No. Paper AAS 99-360, Girdwood, Alaska, August 16-19 1999.
[31] P. A. Finlayson, "PTool Version 1.0 Documentation," Tech. Rep. Jet Propulsion Laboratory, July 1999.
[32] D. J. Grebow, A. E. Petropoulos, and P. A. Finlayson, "Multi-Body Capture to Low-Altitude Circular Orbits at Europa," *AAS/AIAA Astrodynamics Specialist Conference*, No. AAS 11-427, Girdwood, Alaska, July 31 - August 4 2011.
[33] M. W. Lo, "The Interplanetary Superhighway and the Origins Program," *Aerospace Conference Proceedings (2002), IEEE*, Vol. 7, 2001, pp. 3543–3562.
[34] W. S. Koon, M. W. Lo, J. E. Marsden, and S. D. Ross, "Constructing a Low Energy Transfer Between Jovian Moons," *Celestial Mechanics* (A. Chenciner, R. Cushman, C. Robinson, and Z. J. Xia, eds.), 2002, pp. 129–146.
[35] B. F. Villac and D. J. Scheeres, "Escaping Trajectories in the Hill Three-Body Problem and Applications," *Journal of Guidance, Control, and Dynamics*, Vol. 26, March-April 2003, pp. 224–232.
[36] C. v. Kirchbach, H. Zheng, J. Aristoff, J. Kavanagh, B. F. Villac, and M. W. Lo, "Trajectories Leaving a Sphere in the Restricted Three Body Problem," *AAS/AIAA Space Flight Mechanics Meeting*, No. AAS Paper 05-221, Copper Mountain, Colorado, January 23-27 2005.
[37] R. L. Anderson and M. W. Lo, "Virtual Exploration by Computing Global Families of Trajectories with Supercomputers," *AAS/AIAA Space Flight Mechanics Conference*, No. Paper AAS 05-220, Copper Mountain, Colorado, January 23-27 2005.
[38] C. o. t. Planetary Science Decadal Survey, *Vision and Voyages for Planetary Science in the Decade 2013-2022*. Washington, D.C.: The National Academies Press, 2011.
[39] C. Conley, "Low Energy Transit Orbits in the Restricted Three-Body Problem," *SIAM Journal of Applied Mathematics*, Vol. 16, 1968, pp. 732–746.
[40] V. Szebehely, *Theory of Orbits: The Restricted Problem of Three Bodies*. New York: Academic Press, 1967, pp. 7-41.
[41] G. Gómez, A. Jorba, J. Masdemont, and C. Simó, "Study of the Transfer from the Earth to a Halo Orbit Around the Equilibrium Point L_1," *Celestial Mechanics and Dynamical Astronomy*, Vol. 56, August 1993, pp. 541–562.
[42] T. Parker and L. O. Chua, *Practical Numerical Algorithms for Chaotic Systems*. New York: Springer-Verlag, 1989, pp. 130-166.
[43] S. Wiggins, *Introduction to Applied Nonlinear Dynamical Systems and Chaos*, Vol. 2 of *Texts in Applied Mathematics*. New York: Springer-Verlag, 2nd ed., 2003, pp. 28-70.
[44] A. E. Roy and M. W. Ovenden, "On the Occurrence of Commensurable Mean Motions in the Solar System. The Mirror Theorem," *Monthly Notices of the Royal Astronomical Society*, Vol. 115, 1955, pp. 296–309.
[45] A. Miele, "Theorem of Image Trajectories in the Earth-Moon Space," *Astronautica Acta*, Vol. 6, No. 51, 1960, pp. 225–232.
[46] K. C. Howell and J. V. Breakwell, "Three-Dimensional, Periodic, 'Halo' Orbits," *Celestial Mechanics*, Vol. 32, January 1984, pp. 53–71.
[47] J. Masdemont and J. M. Mondelo, "Notes for the Numerical and Analytical Techniques Lectures (draft version)," Advanced Topics in Astrodynamics Summer Course, Barcelona, July, 2004, http://www.ieec.fcr.es/astro04/notes/analnum.pdf, July 2004.
[48] G. Gómez, J. Llibre, M. R., and C. Simó, *Dynamics and Mission Design Near Libration Points Vol. I Fundamentals: The Case of Collinear Libration Points*, Vol. 2 of *World Scientific Monograph Series in Mathematics*. New Jersey: World Scientific, 2001.
[49] W. S. Koon, M. W. Lo, J. E. Marsden, and S. D. Ross, *Dynamical Systems, the Three-Body Problem and Space Mission Design*. Springer, 2008 (to appear).
[50] B. T. Barden and K. C. Howell, "Fundamental Motions Near Collinear Libration Points and Their Transitions," *The Journal of the Astronautical Sciences*, Vol. 46, October-December 1998, pp. 361–378.
[51] E. J. Doedel, R. C. Paffenroth, H. B. Keller, D. J. Dichmann, J. Galán-Vioque, and A. Vanderbauwhede, "Computation of Periodic Solutions of Conservative Systems with Application to the 3-Body Problem," *International Journal of Bifurcation and Chaos*, Vol. 13, No. 6, 2003, pp. 1353–1381.
[52] C. D. Murray and S. F. Dermott, *Solar System Dynamics*. Cambridge, United Kingdom: Cambridge University Press, 1999, pp. 421-428.
[53] R. A. Broucke, "Periodic Orbits in the Restricted Three-Body Problem With Earth-Moon Masses," Technical Report 32-1168, Jet Propulsion Laboratory, February 15 1968.
[54] R. L. Anderson, "The Use of Invariant Manifolds in the Design of Flybys and Endgame Scenarios," Presentation at the Jet Propulsion Laboratory, March 19 2010.
[55] R. L. Anderson and J. S. Parker, "A Survey of Ballistic Transfers to the Lunar Surface," *Journal of Guidance, Control, and Dynamics (to appear)*.